GEOPHYSICS, VOL. XXIV, NO. 4 (OCTOBER, 1959), PP. 790-816, 16 FIGS.

INDUCED POLARIZATION, A STUDY OF ITS CAUSES*

DONALD J. MARSHALL† AND THEODORE R. MADDEN‡

ABSTRACT

The causes of induced electrical polarization include not only the polarization of metal-solution interfaces, but also effects associated with the coupling of different flows. Electro-osmotic, thermal electric, and ion diffusion effects are among such examples. A study of the physical properties of geologic materials indicates that only electrode interface and diffusion flow phenomena are important sources of induced polarization effects.

It was attempted to find characteristic differences between these two phenomena. Theoretical and experimental considerations show that the kinetic processes involved are quite similar in the two cases. This leads to difficulties in identifying the polarizing agent from electrical measurements, although the effects of well mineralized zones are easily recognized.

INTRODUCTION

During the past ten years an increasing interest has developed around the geophysical applications of electrical measurements that go under the popular name of induced polarization measurements.[1] The primary motivation has been the application of these measurements to the detection of sulphide mineralization. It is believed that the phenomenon taking place when electric current passes through a mineralized zone is essentially the same phenomenon that occurs at a polarized electrode (Bleil, 1953).

A polarized electrode is one that hinders the flow of electric current between the electrode and the solution in which it is immersed. Chemical or electrochemical barriers exist which the current carriers must overcome in order to allow current flow to pass across the electrode-liquid interface. Forcing a net current flow to take place across this interface entails an added voltage drop above and beyond that needed to overcome the ohmic losses in the solution and in the electrode. This additional voltage is called the overvoltage.

The picture that is used to explain the induced polarization effects in mineralized rocks involves the ionic current flow in the rock polarizing the metal particles within the rock. When the inducing current is turned off, the overvoltages that were set up fall off with time. Since it also takes a finite time to build up these overvoltages, one finds that the impedance of these zones decreases with increasing frequency, so that the measurements can also be made in the frequency domain. Qualitatively then, these effects behave somewhat as the ordinary

* Manuscript received by the Editor February 6, 1959.

† Nuclide Analysis Associates, State College, Pa.

‡ Dept. of Geology and Geophysics—M.I.T.

[1] The term induced polarization is perhaps a poor one, because it has so many different connotations. It would be more descriptive if we used the expression, induced electrical interfacial polarization, but we shall not attempt to force such a tongue-twisting term on our fellow geophysicists. In any case the measurements involve the transient or frequency dependent electrical properties of the ground.

dielectric property of the materials. These effects, however, occur at audio and sub-audio frequencies which are much too low for the ordinary displacement currents to be of any significance. Irrespective of the origin of the phenomenon, any time dependent or frequency dependent behavior of the electrical impedance of rock materials at these low frequencies is referred to as an induced polarization effect.

INDUCED POLARIZATION MEASUREMENTS AND PARAMETERS

Before going on to the more general study of the possible causes of these effects, it seems worthwhile at this point to review some of the measurement techniques and to correlate the widely different ways of describing the observed polarization effects that are in current use. Results of field measurements will also be presented to demonstrate the usefulness of these measurements in mining exploration.

Several different techniques are used to measure these effects, and several different parameters are used to describe the results of these measurements. When the measurements are made in the time domain, it is a common procedure to turn the current source on for a period, and then turn it off for a period before starting a new cycle with opposite polarity. The voltage remaining just at the beginning of the off-period, or at some fixed interval later, is often measured and compared with the on-period voltage. The polarization is evaluated in terms of mv/volt. Another practice consists of integrating the off-period voltage. The polarization effects are then evaluated in terms of mv-sec/volt.

When the measurements are made in the frequency domain it is the usual practice to compare the impedance at some alternating frequency with that of some very low frequency which is often referred to as the dc impedance. The effect is then evaluated as a certain percentage increase in the conductance at the ac frequency. Sometimes phase shift measurements are made. These phase shifts are usually very small, of the order of one degree or less.

The significance and the interrelation of these varied parameters can be better understood if the ideas used to describe the polarization of a mineralized zone are transcribed into an equivalent circuit (see Figure 1).

In Figure 1, R' stands for the impedance of the complete rock section. It is made up of unblocked ionic conduction paths, R, in parallel with other paths, Z, which are blocked by metallic or semi-conducting minerals. R_m stands for the resistance of the electronic conducting minerals, and R_e stands for the resistance of the electrolytes in the blocked pore paths. C is the electrode capacitance and R_{chem} represents the hindrance to the transfer of electrons between the metallic mineral and the solution.

Because time and frequency domain data are related to each other, when the phenomenon is linear, through the Fourier transform, we can expect to derive frequency information from the transient measurements or vice versa. There is not an exact one to one correspondence between a point in the frequency domain,

and a point in the time domain, but there is often an approximate one. The percentage frequency effect and the mv/volt parameters are found to be closely related (Madden and Marshall, 1958). If the percentage decrease in impedance is used instead of the percentage increase in conductivity, the relationship is given as percent effect at frequency $f_i \cong 0.1$ mv/volt value at $t_i = 1/2\pi f_i$.

The integrated decay voltage is a little different. It is not unlikely that $R_{\text{chem}} \gg R_m + R_e$, so that the dc impedance of $Z = Z(0)$ is approximately equal to R_{chem}. If we make this assumption, and if the integration is carried out long enough, we have that the mv-sec/volt value $= 1{,}000$ CR.

In all these parameters we have a large role played by R, the resistance of the unblocked paths. Small values of R can short circuit the polarizing effects,

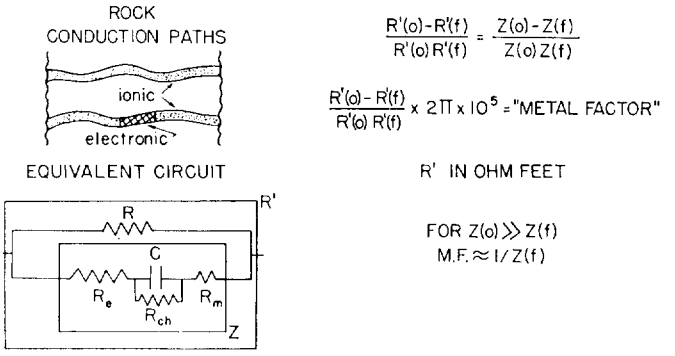

FIG. 1. Diagrammatic representation of section of conducting paths in rock, and the equivalent circuit.

resulting in very small parameter values, while a very tight rock may give large frequency effects without many metallic minerals being present. Since R is in parallel with Z it would seem advisable to look at the change in conductivity of R', for this is just the change in conductivity of Z. When the measurements are made in the frequency domain, this is simply done, and is equal to the frequency effect divided by the dc resistivity. To give reasonably sized values, this parameter is defined as $2\pi[R'(0)-R'(f)]\times 10^5/R'(0)R'(f)$ when using units of ohm-feet for the resistivity. It is called the "metal factor" because of its correlation with metallic mineral content. Using the assumptions previously mentioned concerning the parameters of Figure 1, the metal factor, m.f. $\cong 2\pi \times 10^5/Z(f)$, and is therefore proportional to the ac conductivity of those paths that are blocked off by metallic minerals. The more metal a rock contains, the more paths that will be blocked, and thus the higher the metal factor. As the metallic content continues to increase, the individual paths will have higher ac conductivities, and this two-fold effect starts to skyrocket upwards the values of the metal factor. This is helpful in increasing the signal-to-noise ratio between

the effect of well mineralized zones, and the effect of only slightly mineralized zones. This parameter does favor the rocks having conductive electrolytes in the pores, and thus it is not quite so useful when dealing with sedimentary rocks.

Some typical metal factor values evaluated at 10 cps encountered in igneous areas are shown in Table I.

Similar parameters can be evaluated from the transient measurements. The only one that seems to be used is derived by dividing the mv-sec/volt value by the resistivity. This parameter is essentially proportional to C, the interfacial capacitance per unit cube, but is more often referred to as the effective zero frequency dielectric constant. The frequency measurements could also be evaluated in terms of an effective dielectric constant, but we specifically wish to avoid the

TABLE I

COMMON METAL FACTOR VALUES (10 cps)

Rock Type and Mineralization	Metal Factors
unmineralized granites	<1
unmineralized basic rocks	1–10
finely disseminated sulphides	10–100
disseminated sulphides (1–3%)	100–1,000
fracture filling sulphides (3–10%)	1,000–10,000
massive sulphides	>10,000

use of the term dielectric constant in describing these effects. First of all this so-called effective dielectric constant is not constant, but varies widely as a function of frequency. Secondly, the huge values obtained at low frequencies seem to imply a rather anomalous dielectric phenomenon, while actually the only really anomalous phenomenon is associated with the resistive properties. The interfacial capacitance C is quite large, being of the order of 30 $\mu f/cm^2$, but is not anomalous since the interfacial layer is so thin. The anomalous feature of this layer is its high resistance, despite the fact that it is very thin. If it were not for this high resistance, the interfacial capacitance, which is no different from the capacitance of a similar thickness of ordinary fluid, would play no role.

In the remainder of this paper the polarizing effects will be referred to the frequency domain, and we shall speak of percentage frequency effects and metal factors.

FIELD RESULTS

The increased resolving power of induced polarization measurements over ordinary resistivity measurements in detecting sulphides is demonstrated by some field examples shown in Figures 2–7. The data were taken using 100 ft dipoles for both the sender and receiver. The data are plotted with the abscissa representing the separation between sender and receiver, and the ordinate repre-

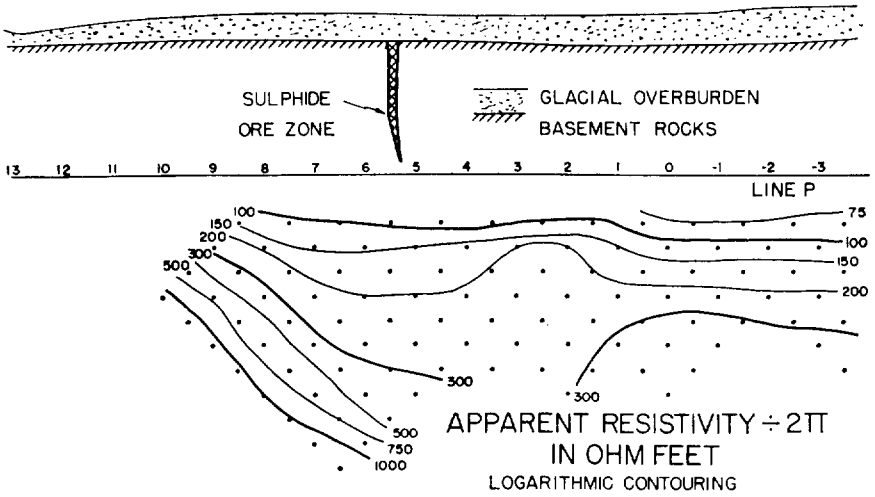

FIG. 2. Resistivity measurements using colinear dipoles.

senting the center position of the spread. In this way a sort of cross-section of the measured apparent electrical parameters are presented. Of course it is not an exact mapping, but it bears certain similarities (Hallof, 1957). The actual measured values have not been shown, merely being represented by dots, but the contours of these values are drawn in. In all these examples there is a clear cut advantage to the induced polarization measurements.

The frequency spectrum of these induced polarization effects are spread out smoothly enough so that the impedance, even though varying with frequency, remains almost purely resistive at any one frequency. This allows one to use

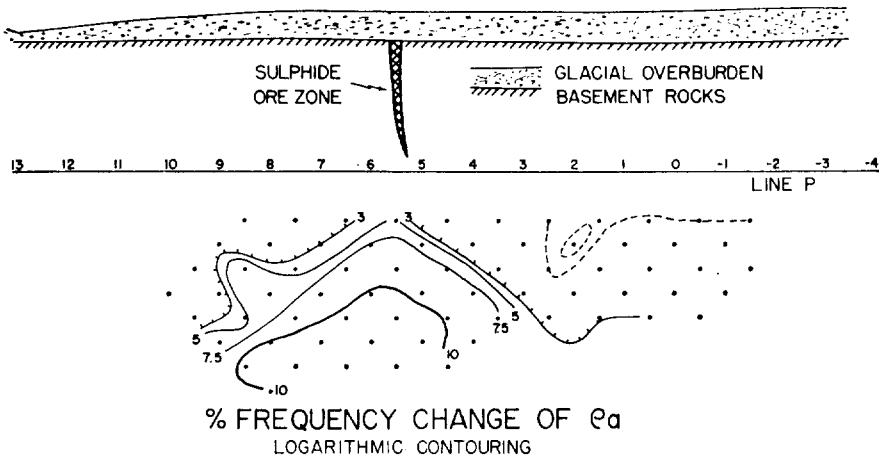

FIG. 3. Frequency variations of apparent resistivity at 60 cps.

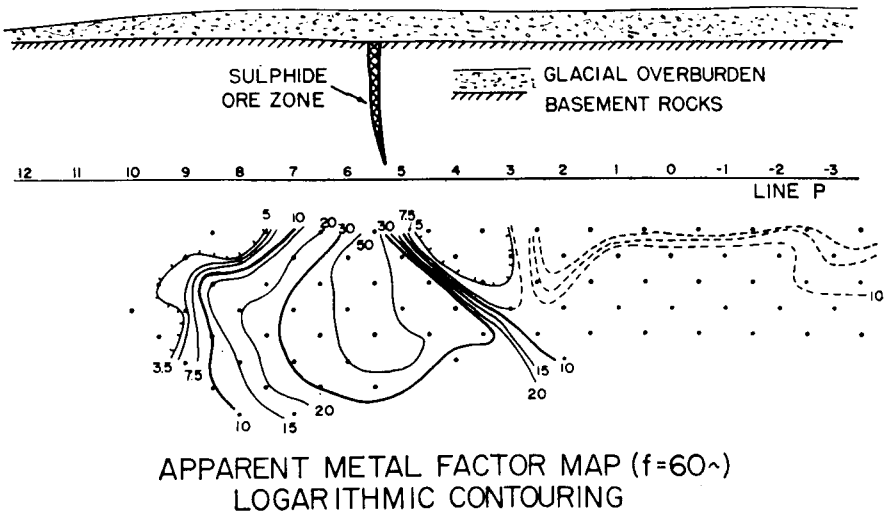

FIG. 4. Metal factor values computed from field measurements.

ordinary resistivity type curves to predict or interpret the apparent polarization effects of a given zone (Hallof, 1957).

COMPLICATIONS TO THE SIMPLE THEORY

The application of induced polarization measurements to the detection of sulphide mineralization is not as simple as it has been assumed in the previous discussion. One reason, of course, is that other semi-conducting minerals such as graphite, magnetite, and pyrolusite cause similar polarization effects. Polari-

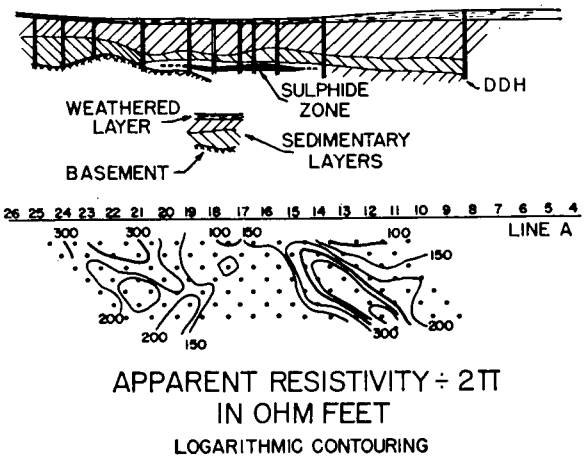

FIG. 5. Resistivity measurements using colinear dipoles.

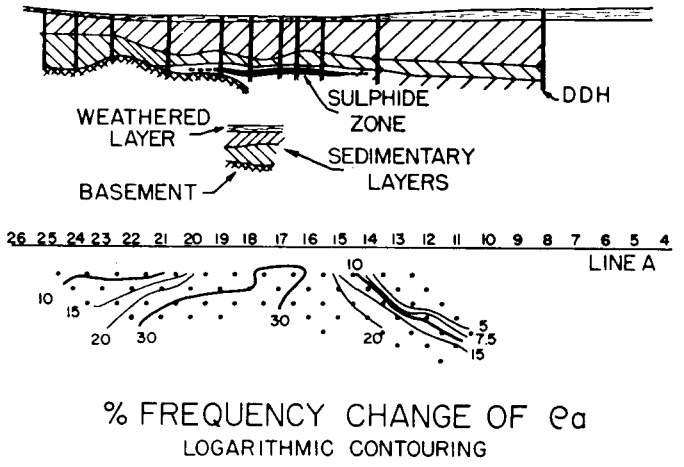

FIG. 6. Frequency variations of apparent resistivity at 60 cps.

zation can also occur, however, without the presence of any semi-conducting minerals. Schlumberger, in perhaps the first reference to induced polarization methods, stated that background polarization effects drowned out the effect of the sulphide minerals (Schlumberger, 1920). This view is somewhat exaggerated, but Vacquier in his work showed that clay minerals could lead to finite polarization effects (Vacquier et al., 1957). Other groups have also been observing these effects (Henkel and Van Nostrand, 1957; Brant, personal communication).

Because of the presence of these complicating factors, this present study was taken up. It was hoped that through an increased understanding of the causes of induced polarization in geologic materials, one could better interpret the electri-

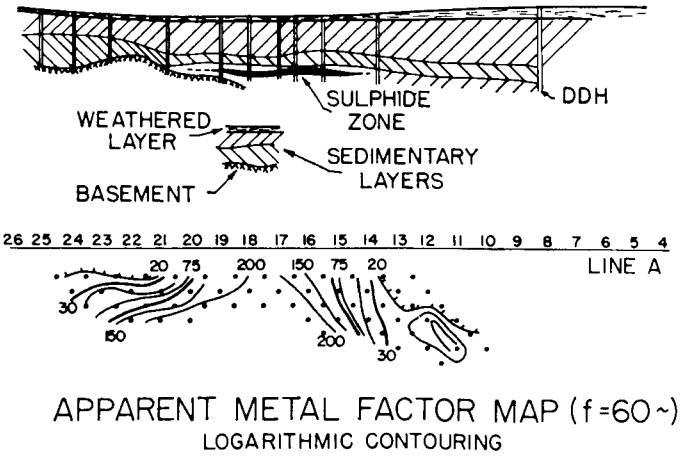

FIG. 7. Metal factor values computed from field measurements.

cal measurements. It seems appropriate then to attack this problem from a fresh point of view, starting with more general concepts rather than a specific model such as that given in Figure 1.

POLARIZATION AS ENERGY STORAGE

The observation that we have is that the polarizable materials are capable of maintaining, for a certain time, an electric current flow after an applied current field is turned off. Actually what is observed is a voltage gradient, and this does not guarantee that electric current is flowing, as will be apparent later, but some sort of flow will be taking place. This is a manifestation that energy is stored in the medium when current is passed through, and usually at least some of this energy is released by maintaining electric current flow after the driving field is turned off. The five ordinary forms of energy storage are, electric, magnetic, mechanical, thermal, and chemical. It is conceivable that any one or all of these are involved in the phenomenon. The picture presented in Figure 1 assumed that the energy was stored as electric energy in the capacitor C. This is the simplest and most direct form of setting up an electric polarization effect.

Another obvious form of energy storage is in the magnetic field. It is known that an electric current always sets up a magnetic field, and that when the current is turned off, the collapsing magnetic field returns its stored energy back into electrical energy. This effect can be very complicated when the geometry of the current flow is irregular, but for simple half-space geometries the solutions are well known (Sunde, 1949). When colinear spreads are used to make the field measurements, these electromagnetic effects behave qualitatively much like the polarization effects of mineralized zones. A two-fold increase of apparent conductivity takes place as the frequency is increased. The frequencies at which the effect is observed, however, are usually quite high, unless large separations in conductive areas are involved. For a separation of 2,000 ft in an area whose resistivity is 300 ohm-ft, no appreciable effect is observed until frequencies of 10 cps or higher are used. When the ground conductivities are not homogeneous, the electromagnetic effects can become quite different. This is especially true when horizontal variations of conductivity exist. Measurements have been made in the field where the apparent resistivity increased by more than three fold as the frequency was increased (Madden et al., 1957). These effects are again limited to the higher frequencies, however.

POLARIZATION THROUGH THE COUPLING OF FLOWS

The electromagnetic effects can be avoided, as has been mentioned, by using low enough frequencies, but anomalous polarization effects are still found when low frequencies are used. The possible effects of mechanical, thermal, and chemical energy storage must be investigated therefore. To store energy in these forms, a coupling must exist between the electric current flow and other flows such as heat and matter. The existence of such a coupling will then allow the stored

energy on its release to cause electric current flow again, and thus the phenomenon will be a form of induced electric polarization. A simple illustration of this idea is given in Figure 8. For instance, through electro-osmotic coupling, an electric current flow will cause a solvent flow through a capillary system. This flow may build up a hydrostatic pressure, either by building up a hydrostatic head against gravity, or perhaps through the blocking action of an impermeable bed. When the electric current is turned off, the hydrostatic pressure built up will drive the solvent back, and the solvent flow in turn will cause an electric current flow.

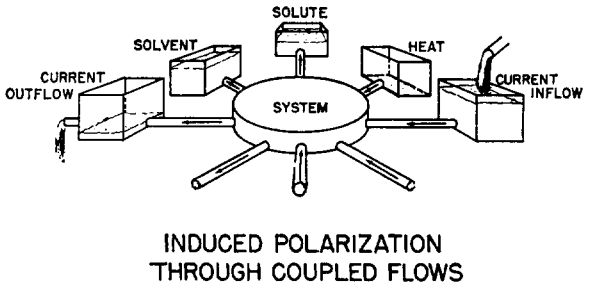

FIG. 8. Pictorial representation of the coupling of flows and the development of counter forces in a system.

This flow almost immediately builds up an electric potential which opposes any further current flow, and which is observed as a polarization voltage.

In a similar way any heat flow induced by the current flow can store energy thermally if temperature differences are set up. The solute flow can cause concentration differences to build up, and this represents a chemical energy.

The study of such couplings and their interrelations is the main area of investigation of steady-state thermodynamics. According to the principles of steady-state thermodynamics, the equations describing a general electrolyte system with coupling are[2]

$$\begin{matrix}\text{flow cations} \\ \text{flow anions} \\ \text{flow solvent} \\ \text{flow heat}\end{matrix} = \begin{bmatrix} J_p \\ J_n \\ J_s \\ J_q \end{bmatrix} = \begin{bmatrix} L_{11}L_{12}L_{13}L_{14} \\ L_{21}L_{22}L_{23}L_{24} \\ L_{31}L_{32}L_{33}L_{34} \\ L_{41}L_{42}L_{43}L_{44} \end{bmatrix} \begin{bmatrix} -\nabla\mu_p - FZ_p\nabla\phi \\ -\nabla\mu_n - FZ_n\nabla\phi \\ -\nabla P \\ -\nabla T/T \end{bmatrix} \tag{1}$$

where

ϕ = electric potential; μ = chemical potential; P = pressure;
T = temperature; $L_{ij} = L_{ji}$; F = Faraday's constant; and Z = ion valence.

[2] This is not the form of these equations usually found, but we follow Eckart here in an attempt to avoid the presence of arbitrary potential terms that appear in the formulations given in Denbigh and DeGroot (Eckart 1940, Denbigh 1951, DeGroot 1952).

The column on the left represents the flow vectors, while the column on the right of (1) represents the generalized forces. The L_{ij} matrix consists of the terms relating to the properties of the media such as the conductance and permeability.

These relationships assume a linear behavior of the medium, and this is always observed for small-flow densities. Onsager's relationships, $L_{ij}=L_{ji}$, is based on extensions of thermodynamics to situations involving slight deviations from equilibrium. It also appears to be verified experimentally for small-flow densities. This relationship is of great help in organizing the experimental results.

From these relationships the possible magnitudes of electrical polarization can be deduced in terms of the coupling coefficients. Many of these coefficients are well known from other studies. For instance, the solvent-electric current flow coupling known as electro-osmosis or streaming potential has been studied by geophysicists because of the effects on self-potential logging (Wylie, 1955). The soil mechanics engineers also have made such studies because of the possible applications in soil consolidation (Casagrande, 1952).

The thermo-electric properties are not as well known, although at present a great effort is being made to develop efficient thermo-electric materials because of their possible use in energy conversion. The measure of this efficiency is exactly the same parameter that evaluates its induced polarization capabilities. These studies are concentrating on semi-conducting materials. It is quite apparent, from data to be shown later, that geologic materials do not have the required properties.

The coupling effects between solute flow and electric currents are also very well known, being an important part of the subject matter of electro-chemistry. These effects are familiar to geophysicists using self-potential measurements, for they are represented by the familiar diffusion potential phenomena.

ELECTRO-OSMOTIC COUPLING

To investigate the possible influence of electro-osmotic coupling on induced electrical polarization we can rewrite equation (1), assuming that all the induced forces except ∇P are zero, and ignoring any dependence of μ on pressure. We also combine J_p and J_n to give us the current flow I.

$$\begin{aligned} I = F(Z_pJ_p + Z_nJ_n) = &- F^2[L_{11}Z_p^2 + L_{22}Z_n^2 + (L_{12} + L_{21})Z_pZ_n]\nabla\phi \\ &- F(L_{13}Z_p + L_{23}Z_n)\nabla P \end{aligned} \tag{2}$$

$$J_s = - F(L_{31}Z_p + L_{32}Z_n)\nabla\phi - L_{33}\nabla P. \tag{3}$$

In the ultimate steady-state a hydrostatic pressure will build up to prevent any further electro-osmotic solvent flow. The pressure gradient needed to prevent the solvent flow can be calculated from (3) by setting $J_s=0$. When this pressure gradient is introduced into (2) we obtain, using Onsager's relationship $L_{ij}=L_{ji}$,

$$I(\text{steady-state}) = -\left\{F^2[L_{11}Z_p^2 + L_{22}Z_n^2 + (L_{12} + L_{21})Z_pZ_n] - \frac{F^2(L_{13}Z_p + L_{23}Z_n)^2}{L_{33}}\right\}\nabla\phi. \tag{4}$$

The term multiplying $-\nabla\phi$ is the effective conductivity in the steady-state, σdc. If high frequencies are used, no pressure gradient can build up, and from (2) we have that the high frequency conductivity is

$$\sigma_{ac} = F^2[L_{11}Z_p^2 + L_{22}Z_n^2 + (L_{12} + L_{21})Z_pZ_n]. \tag{5}$$

The maximum frequency effect is given by

$$\frac{\sigma_{ac}}{\sigma_{dc}} = \frac{1}{[1 - F^2(L_{13}Z_p + L_{23}Z_n)^2/\sigma_{ac}L_{33}]}. \tag{6}$$

The coefficients used are not the parameters in common usage. The streaming potential, which represents the potential induced by an applied pressure gradient, can be given in terms of these same coefficients, however.

$$\left(\frac{\nabla\phi}{\nabla P}\right)_{I=0} = \xi = -F(L_{13}Z_p + L_{23}Z_n)/\sigma_{ac}. \tag{7}$$

Thus it is possible to rewrite (6) as

$$\frac{\sigma_{ac}}{\sigma_{dc}} = 1\Big/\left[1 - \frac{\xi^2\sigma_{ac}}{L_{33}}\right]. \tag{8}$$

The maximum polarization effect can, therefore, be determined in terms of the conductivity, the permeability, and the streaming potential, which are all easily measured parameters. In Table II are given some results of such measurements on geologic materials.

TABLE II

MEASURED ELECTRO-OSMOTIC COUPLING COEFFICIENTS AND POSSIBLE POLARIZATION EFFECTS

Sample	Streaming Potential mv/atm.	Maximum % Frequency Effect	Investigator
quartz s.s.	8	.03	Kermabon
quartz s.s.	9	.0002	Kermabon
red s.s.	5.5	.02	Kermabon
shale	1	.05	Kermabon
limestone	2	.03	Kermabon
kaolinite (dispersed, Na)	30	2.0	Olsen
kaolinite (natural flocculated, Ca)	17	.02	Olsen
kaolinite (flocculated, .1 N NaCl)	0.7	.007	Olsen

The values listed in the table indicate that the electro-osmotic effects are relatively unimportant in causing induced electrical polarization.

THERMO-ELECTRIC COUPLING

A very similar analysis can be carried out to investigate the possible influence of thermo-electric effects. The thermo-electric coupling is more complicated because of the role played by the chemical potentials, which depend both on the temperature and on the concentration of the solute. In general, unlike the electro-osmotic case, to evaluate the polarization contribution it would be necessary to measure both cross-coupling effects; the thermally induced potential gradients and the electrically induced thermal gradients.

If we ignore pressure effects

$$\nabla\mu_j = \frac{\partial\mu_i}{\partial T}\nabla T + \sum_j \frac{\partial\mu_i}{\partial C_j}\nabla C_j.$$

The time scale for heat flow at ordinary temperatures is much shorter than the time scale for diffusion flow, so that for certain time scales we can assume the concentrations remain unchanged. This allows us to set

$$\nabla\mu_i \cong -S_i\nabla T = -TS_i\frac{\Delta T}{T} \tag{9}$$

S_i = partial molal entropy.

Our thermal coupling equations can then be written as

$$I = F(Z_pJ_p + Z_nJ_n) = -F^2[Z_p^2L_{11} + Z_n^2L_{22} + Z_pZ_n(L_{12} + L_{21})]\Delta\phi$$
$$- F[L_{14}Z_p + L_{24}Z_n - (Z_pL_{11} + Z_nL_{21})TS_p - (Z_nL_{22} + Z_pL_{12})TS_n]\frac{\nabla T}{T} \tag{10}$$

$$J_Q = -F[Z_pL_{14} + Z_nL_{24}]\nabla\phi - [L_{44} - L_{41}TS_p - L_{42}TS_n]\frac{\nabla T}{T}\cdot \tag{11}$$

The quantity $-F[Z_pL_{14}+Z_nL_{24}]\nabla\phi$ appearing in (11) can be interpreted as the heat transported by the ions moving under the influence of the electrical field.

$$-F[Z_pL_{14} + Z_nL_{24}]\nabla\phi = Q_pJ_p + Q_nJ_n. \tag{12}$$

Q = heat of transport.

From the definition of transference number,

$$\tau^+ = FZ_pJ_p/I; \qquad \tau^- = 1 - \tau^+ = FZ_nJ_n/I$$

we have therefore

$$FZ_pL_{14} = Q_p\tau^+\sigma_{ac}/FZ_p \tag{13}$$

$$FZ_nL_{24} = Q_n\tau^-\sigma_{ac}/FZ_n. \tag{14}$$

We also have from (10)

$$F(Z_pL_{11} + Z_nL_{12}) = \tau^+\sigma_{ac}/FZ_p \tag{15}$$

$$F(Z_nL_{22} + Z_pL_{21}) = \tau^-\sigma_{ac}/FZ_n. \tag{16}$$

A further simplification of notation is achieved by setting

$$[L_{44} - TS_pL_{41} - TS_nL_{42}] = TK; \qquad K = \text{thermal conductivity.} \tag{17}$$

We can now rewite (10) and (11), using Onsager's relation $L_{ij}=L_{ji}$, as

$$I = -\sigma_{ac}\nabla\phi - \left[(Q_p - TS_p)\frac{\tau^+}{FZ_p} + (Q_n - TS_n)\frac{\tau^-}{FZ_n}\right]\sigma_{ac}\frac{\nabla T}{T} \tag{18}$$

$$J_Q = -\left(Q_p\frac{\tau^+}{FZ_p} + Q_n\frac{\tau^-}{FZ_n}\right)\sigma_{ac}\nabla\phi - K\nabla T. \tag{19}$$

In the steady-state limit $J_q=0$, and solving for the temperature gradient set up we can obtain the steady-state conductivity.

$$\sigma_{dc} = \sigma_{ac}\left[1 - \frac{\left(\sum Q_i\frac{\tau_i}{FZ_i}\right)\left(\sum (Q_i - TS_i)\frac{\tau_i}{FZ_i}\right)\sigma_{ac}}{TK}\right]. \tag{20}$$

If the time scale is extended, the temperature gradients can also establish concentration gradients (Soret effect) which will modify the current flow because of the diffusion potentials set up. A greater practical difficulty in establishing the magnitudes of these effects is the fact that a measurement of the thermo-electric coefficient

$$\theta = \left(\frac{\nabla\phi}{\nabla T}\right)_{I=0} = -\sum\left(\frac{Q_i - TS_i}{T}\right)\frac{\tau_i}{FZ_i} \tag{21}$$

is not enough to establish the polarization effects of this coupling. In principle one would need to also measure the heat of transport. Such a calorimetric measurement is much more difficult to carry out than the electrical measurement involved in (21).

We can make estimates of the term $\sum Q_i(\tau_i/FZ_i)$ in (20) which are adequate for our purposes here. In most rocks the positive ion transference number is much larger than the negative ion transference number. Thus

$$\theta \cong \frac{Q_p - TS_p}{TFZ_p}. \tag{22}$$

The partial molal entropies for aqueous solutions of ions are known, so that if we can assume similar values for the ions in the pore fluids, (22) would give us an estimate of $\sum Q_i(\tau_i/FZ_i)$. Using KCl solutions typical values of θ ran around 0.3 mv/deg.C. These were measured in a cell where the thermo-electric voltages across the rock samples were bucked against the thermo-electric voltage across a water column (Uhri, 1958). The voltage between the measuring electrodes were then corrected for a semi-theoretical value of the water thermo-electric voltage (Eastman, 1928, and Wirtz, 1948). The partial entropy value for K^+ of 24 entropy units per mole, thus gave from (22) an estimate of Q_{K+} of 3.6 Kcal/mole. The value of $\sum(Q_i - TS_i)\tau_i$ was about 2.3 Kcal/mole, so that we are within the correct order of magnitude to replace $\sum Q_i\tau_i$ by $\sum(Q_i - TS_i)\tau_i$. This allows us to rewrite (20) as

$$\frac{\sigma_{ac}}{\sigma_{dc}} \cong 1 \Big/ \left(1 - \frac{T\theta^2\sigma_{ac}}{K}\right). \tag{23}$$

In Table III are listed some of the thermo-electric data and the approximate maximum polarization effect possible from such coupling.

TABLE III

MEASURED THERMO-ELECTRIC COUPLING COEFFICIENTS AND POSSIBLE POLARIZATION EFFECTS

Sample	Thermo-Electric Coef. mv/deg. C	Maximum % Frequency Effect
ss. with clay	.23	.000003
s.s.	.48	.00003
shale	.33	.00004
limestone	.27	.0000002

It is obvious that this coupling is of no importance in causing polarization effects. Actually the thermo-electric coefficients are quite high, but the ratio of electrical conductivity to thermal conductivity is very low, so that from (23) $\sigma_{ac} \cong \sigma_{dc}$. This is also the reason why semi-conductors are being used for thermo-electric power conversion; one must have a very good electrical conductor as well as strong thermo-electric effects.

DIFFUSION COUPLING

It is apparent by now that the cross terms appearing in the matrix describing the flow properties of the medium are not large enough in geologic materials to cause appreciable polarization effect. It is quite a different matter, however, when diffusion flow effects are investigated. This, of course, is because the ions themselves carry the electric current, so that the diffusion gradients and the electrical potential gradients have to appear together as primary driving forces for the ion motion.

If we drop all the off diagonal terms in (1) we are left with

$$J_p = - L_{11}\nabla\mu_p - L_{11}FZ_p\nabla\phi \tag{24}$$

$$J_n = - L_{22}\nabla\mu_n - L_{22}FZ_n\nabla\phi \tag{25}$$

as the flow equations for the anions and the cations. In place of the coefficients L_{ij}, we can introduce the more familiar electrochemical quantities of mobility, diffusion coefficients, and transference numbers. Thus we can rewrite the flow equations, assuming uni-valent ions, as

$$J_p = - D_p \frac{\partial p}{\partial x} + u_p pE \tag{26}$$

$$J_n = - D_n \frac{\partial n}{\partial x} - u_n nE \tag{27}$$

U = mobility — p = cation concentration

D = diffusion coef. — n = anion concentration

$t^+ = U_p/(U_p + U_n) = D_p/(D_p + D_n)$ = cation transference no.

$t^- = 1 - t^+$ = anion transference no.

If t^+ should vary along the current path, a divergence will result in the flow of the ions, causing concentration gradients to build up. This is illustrated in Figure 9 where zone II represents a strongly cation selective zone, and zone I represents a zone with no selectivity. Because of its selective transference properties zone II would be called a membrane zone. Since the current in zone II is largely carried by the cations, a surplus of these ions will occur at one end of zone II, and a deficiency at the other end. The anion flow will also be unbalanced, and the buildup of anions will equal that of the cations. The resulting concentration gradients will modify the ion flow until a balance is reached. In this steady-state

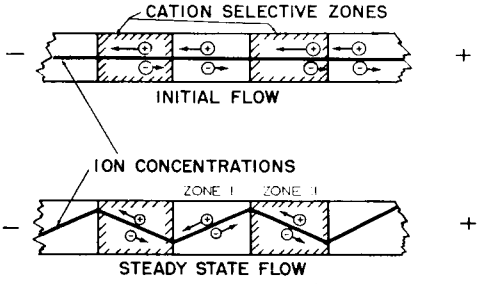

FIG. 9. Ion motion and concentration changes developed by current flow through a membrane system.

condition the net flow of cations and anions in zone II will equal that in zone I.

$$J_{p\mathrm{I}} = J_{p\mathrm{II}} \tag{28}$$

$$J_{n\mathrm{I}} = J_{n\mathrm{II}}. \tag{29}$$

The impedance of the zones will also be modified, because the concentration gradients developed will have diffusion potentials associated with them. These potentials arise because of a slight unbalance of charge , but since so little charge is needed to develop an electric field, one can say that the cation and anion concentrations are essentially equal.

$$p = n. \tag{30}$$

The electric field is assumed to be constant in each zone, so that the total potential difference across the pair of zones is given by

$$\Delta\phi = -E_{\mathrm{I}}\Delta L_{\mathrm{I}} - E_{\mathrm{II}}\Delta L_{\mathrm{II}}. \tag{31}$$

The concentrations, p and n, will be continuous across the boundaries, so that if the succeeding zones repeat the same pattern with the same geometry and electrical properties, we can put

$$\Delta p_{\mathrm{I}} = -\Delta p_{\mathrm{II}} \tag{32}$$

$$\Delta n_{\mathrm{I}} = -\Delta n_{\mathrm{II}}. \tag{33}$$

When it is also assumed that the concentration gradients are constant in each zone, (28), (29), (30), (32), and (33) can be considered as a system of algebraic equations for the unknown electric fields and concentration gradients. Solving these we obtain for the steady-state conductance

$$\sigma_{\mathrm{dc}} = \frac{Fu_{p\mathrm{I}}C\left(\dfrac{1}{\tau_{\mathrm{II}}^{-}} + \dfrac{A}{B}\dfrac{1}{\tau_{\mathrm{I}}^{-}}\right)S_{\mathrm{I}}S_{\mathrm{II}}}{\Delta L_{\mathrm{I}}\left[S_{\mathrm{I}}\left(1 + \dfrac{B}{A}\right) + S_{\mathrm{II}}\left(1 + \dfrac{A}{B}\right)\right]} \tag{34}$$

$$c = \text{net concentration}$$

$$A = \Delta L_{\mathrm{I}}/\Delta L_{\mathrm{II}}$$

$$B = D_{p\mathrm{I}}/D_{p\mathrm{II}}$$

$$S_i = \tau_i^{-}/\tau_i^{+}.$$

At the high frequency limit, no concentration gradients develop, and the only unknowns are the potential gradients. Using the condition that the electric current is the same in the two zones as well as the condition on the total voltage given by (31) allows us to solve for the conductance

$$\sigma_{\mathrm{ac}} = Fu_{p\mathrm{I}}CA/\Delta L_{\mathrm{I}}(A\tau_{\mathrm{I}}^{+} + B\tau_{\mathrm{II}}^{+}). \tag{35}$$

TABLE IV

POLARIZATION OF MEMBRANE MODEL

percent frequency effect ($\tau_I^+=0.5$)

τ_{II}^+	$B=$ / $A=$	1 / .1	1 / 1	1 / 10	3 / .1	3 / 1	3 / 10	D_P Ratio Length Ratio
.999		4.8	33	81	1.6	14	62	
.990		4.5	32	67	1.6	14	57	
.909		3.3	20	20	1.2	9.6	27	
.667		.7	2.8	1.2	1.9	1.8	2.5	

The maximum frequency effect that diffusion coupling can develop in our model is given as

$$\frac{\sigma_{ac}}{\sigma_{dc}} = \frac{(A+B)\left[\dfrac{A}{\tau_I^-\tau_{II}^+}+\dfrac{B}{\tau_I^+\tau_{II}^-}\right]}{\left[\dfrac{A}{\tau_{II}^+}+\dfrac{B}{\tau_I^+}\right]\left[\dfrac{A}{\tau_I^-}+\dfrac{B}{\tau_{II}^-}\right]}. \tag{36}$$

Typical values are given in Table IV. It will be observed that there is a finite limit to the frequency effect caused by this form of polarization.

For the time scales to be reasonable, the zones must be very small, and one would not be able to measure the electrical properties of each zone. The presence of membrane zones should make itself known when diffusion measurements are made, because the average transference value for the anions and cations will not be equal, and a diffusion potential will be set up. The information given in Table IV is therefore plotted in Figure 10 in terms of the effective transference number which would be determined from diffusion potential measurements. In Table V are shown the results of diffusion measurements on a few rock samples, and the possible polarizing effects that diffusion coupling could result in.

The values listed above show that these diffusion coupling effects are capable of causing considerable electrical polarization. There are two factors that should be pointed out here. First of all the possible polarization effects could increase without limit if we assumed that zones with positive ion blocking properties

TABLE V

MEASURED TRANSFERENCE VALUES AND POSSIBLE POLARIZATION EFFECTS

Sample	t^+ (Effective)	Maximum % Frequency Effect
tuff	.51	1
tuff	.72	40
tremolite limestone	.87	72
sandstone, medium grained	.48	1
sandstone, medium grained	.49	1
sandstone, fine grained	.89	78
dirty sandstone	.6	20

existed as well as those zones which can block negative ions. It is very unlikely that geologic materials will ever include such zones, but synthetic ion exchange resins can be found that do. The second factor that should be pointed out is the dependence of the polarization effect on the length ratio A. If a material has zones of very high t^+ values, but these zones are too numerous, so that most of the conduction path lies within such zones, little polarization will result. If has been

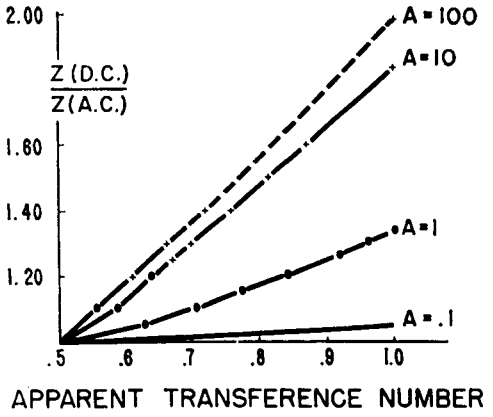

FIG. 10. Effect of the ratio of the zone lengths on the maximum polarization of a membrane system.

noted before that clays, despite their very striking t^+ values, often show extremely little polarization effect, especially if they have been mechanically manipulated. It is believed that this may be due to a tendency for the conduction paths to lie almost entirely within clay zones. Vacquier in his work reported that he could only obtain polarization effects from clays when he coated them on sand grains.

We have advanced no theory here as to why the pores of a rock or clay particles should show much membrane properties. This will involve a microscopic theory of the mineral solution interfaces. It is interesting to point out in this connection, however, that the presence of a surface charge on the minerals does not by itself cause any polarization.

A more detailed study showed that a fixed charge in a system can lead to a very slight polarization, but it is really necessary, if the system is to have a finite polarization effect, that the motion of certain ions be hindered in the system. Thus it appears that the electrostatic and Van der Waal forces that attract the positive ions to the surface of a polarizing clay system must also act to prevent negative ions from moving along the surface.

COMPARISON OF ELECTRODE AND MEMBRANE POLARIZATION

The model given for membrane polarization sets a finite limit to the polarization effect of membrane zones within a rock. The model given in Figure 1 for

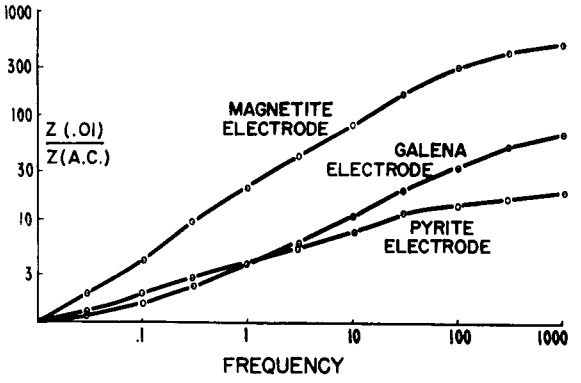

FIG. 11. Impedance of natural electrodes.

electrode polarization is not so limited however. In Figure 11 is shown some data on the interfacial impedance of a few natural electrodes. The frequency effects are much larger than 100 percent. We might expect, therefore, to find a difference between the magnitude of the observed polarization depending on the cause of the polarization. Because of the diluting, mentioned before, that is caused by parallel unpolarized conduction paths, it seems best to compare the metal factors rather than the percentage frequency effects. In Figure 12 there is shown in a somewhat generalized form, the results of laboratory measurements on a large number of rock samples, and field measurements in many areas. These results again indicate the pronounced polarization effects of well-mineralized rocks. However, in rocks with less mineralization, there begins to exist considerable ambiguity. This is especially true in sedimentary rocks of high conductivity. The geometry of the mineralization is also very critical. When the sulphides form connected veinlets

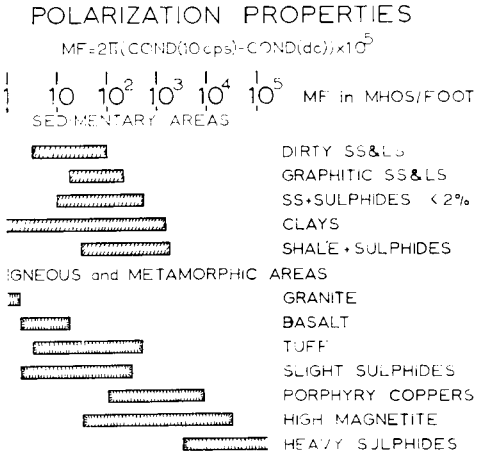

FIG. 12. Distribution of observed metal factor values.

their metal factor values are far superior to those of well-disseminated sulphides.

These results, although not eliminating the great usefulness of induced polarization measurements, do point out certain dangers in holding too simple a concept about the causes of the polarization. It also leads one to search for other criteria, besides a magnitude criterion, to help in separating out the various contributing factors.

FREQUENCY BEHAVIOR OF MEMBRANE POLARIZATION

The mechanism involved in membrane polarization appears to be quite different than that pictured in Figure 1 for electrode polarization. It might be hoped, therefore, that the details of the frequency spectrum for the two polarization effects would lead to some means of distinguishing between the different effects. For this reason the study of the membrane model was expanded.

From equations (26) and (27) we can obtain the equations of motion for the ion species.

$$\frac{\partial p}{\partial t} = D_p \frac{\partial^2 p}{\partial x^2} - U_p \frac{\partial}{\partial x}(pE) \tag{37}$$

$$\frac{\partial n}{\partial t} = SD_p \frac{\partial^2 n}{\partial x^2} + SU_p \frac{\partial}{\partial x}(nE). \tag{38}$$

Poisson's equation must also be satisfied

$$\frac{\partial E}{\partial x} = \frac{F}{\epsilon}(p - n). \tag{39}$$

These equations are non-linear but can be linearized for our case since we are interested in very small current densities. For small current densities we can consider the electric fields and the concentration changes to be small

$$\begin{aligned} P &= C + \Delta P \\ N &= C + \Delta N, \\ E &= \Delta E. \end{aligned} \tag{40}$$

If the product of these small terms is neglected and harmonic time dependence is assumed, (37), (38), and (39) become linear equations for Δp, Δn, and ΔE.

$$i\omega \Delta p = D_p \frac{d^2 \Delta p}{dX^2} - U_p C \frac{d\Delta E}{dX} \tag{41}$$

$$i\omega \Delta n = SD_p \frac{d^2 \Delta n}{dx^2} + SU_p C \frac{d\Delta E}{dx} \tag{42}$$

$$\frac{d\Delta E}{dx} = \frac{F}{\epsilon}(\Delta p - \Delta n). \tag{43}$$

These equations are the ones usually dealt with in treatments of space charge effects, and appear in discussions of solution-electrode interfaces as well as in this membrane model (MacDonald, 1953). The general solutions are simple exponentials with two characteristic lengths.

$$\begin{aligned} \Delta p &= L_p e^{\pm r_1 x} + M_p e^{\pm r_2 x} \\ \Delta n &= L_n e^{\pm r_1 x} + M_n e^{\pm r_2 x}. \end{aligned} \tag{44}$$

One of these characteristic lengths

$$\frac{1}{r_1} = 1/K\left(1 + \frac{j\omega(S+1)}{DSK^2}\right)^{1/2} \cong 1/K; \qquad K^2 = \frac{2CF^2}{\epsilon RT} \gg 1 \tag{45}$$

is essentially frequency independent and represents a space charge set up at the boundaries of a zone. The other characteristic length

$$\frac{1}{r_2} = \left[\frac{2D_p S}{j\omega(S+1)}\right]^{1/2} \tag{46}$$

varies inversely with the square root of the frequency and represents a diffusion phenomenon.

The undetermined constants in the solution are solved for by imposing the boundary conditions. In the membrane model, because of the symmetry imposed by the regular spacing of the zones, there are six constants to be determined, three for each zone. The boundary conditions can be given as the continuity of concentration and of ion flow at the boundary, the continuity of E at the boundary, and the condition that $\int \Delta E dx = -\Delta\phi$, the applied potential. These conditions, when expressed in terms of the general solutions, give us six simultaneous algebraic equations for the undetermined constants. Their solution is straightforward, but laborious, since the system of equations is highly singular and many terms must be carried along. The impedance of the membrane zone can then be determined and is given by

$$Z = \frac{\Delta L_{\mathrm{I}}}{U_{p\mathrm{I}} CF}\left\{ t_{\mathrm{I}}^{+} + \frac{B}{A} t_{\mathrm{II}}^{+} + \frac{(S_{\mathrm{II}} - S_{\mathrm{I}})^2}{\dfrac{X_{\mathrm{I}} S_{\mathrm{I}}}{(t_{\mathrm{II}}^{+})^2 t_{\mathrm{I}}^{+} \tanh X_{\mathrm{I}}} + \dfrac{A}{B}\dfrac{X_{\mathrm{II}} S_{\mathrm{II}}}{t_{\mathrm{II}}^{+}(t_{\mathrm{I}}^{+})^2 \tanh X_{\mathrm{II}}}} \right\}$$

$$X_i = \left(\frac{j\omega}{2D_{pi} t_i^{-}}\right)^{1/2} \frac{\Delta L_i}{2}$$

$$A = \Delta L_{\mathrm{I}} / \Delta L_{\mathrm{II}} \tag{47}$$

$$B = D_{p\mathrm{I}} / D_{p\mathrm{II}}$$

$$S_i = t_i^{-} / t_i^{+}.$$

Values of the membrane impedance as a function of frequency are shown in Figure 13, where it is assumed that zone I is a neutral zone. The value used for

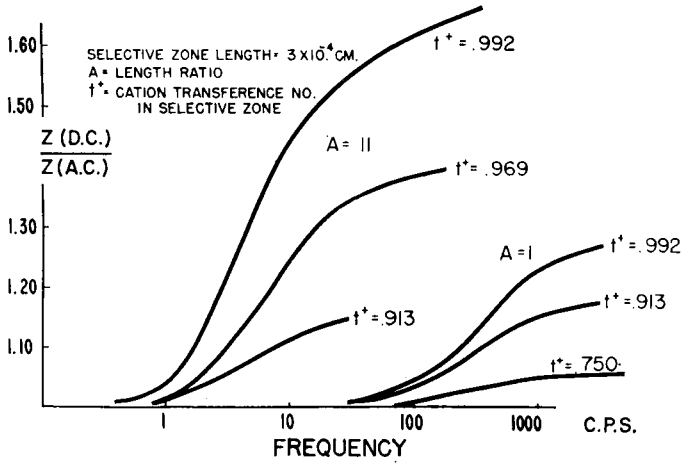

FIG. 13. Details of the impedance of a simple membrane system.

ΔL_2 of 0.3×10^{-3} cm. is typical of the size of clay particles. The frequency response for a given zone size is quite sharp. The frequencies at which the impedance is varying depend on the square of zone length, so that in an actual system with a distribution of zone lengths we can expect the frequency variations to be spread out over a wide range of frequencies. In Figure 14 are shown some impedance measurements on real membrane systems for comparison.

FREQUENCY BEHAVIOR OF ELECTRODE POLARIZATION

To compare electrode polarization to membrane polarization we must extend the simple model of Figure 1. In fact the data shown in Figure 11 are quite different from what we would expect from a simple RC circuit. Therefore, to better under-

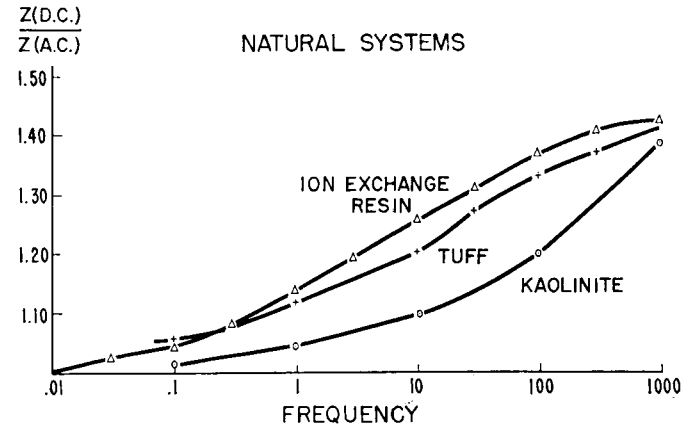

FIG. 14. Details of the impedance of a natural membrane system.

stand the nature of electrode impedances, detailed kinetic calculations were also carried out for the impedance of an electrode-solution interface. Equations (41) (42) and (43) can again be used to describe the ion motions, but the boundary conditions are very different. First of all there can be capacitive coupling between the solution and the electrode. Secondly any Faradaic current involving actual charge transfer must entail chemical reactions, and a whole chain of events may follow depending on the products of these reactions. These events are all reflected in the boundary conditions, and thus modify the electrode impedance (Madden and Marshall, 1959). When typical reaction rate values are used, however, the

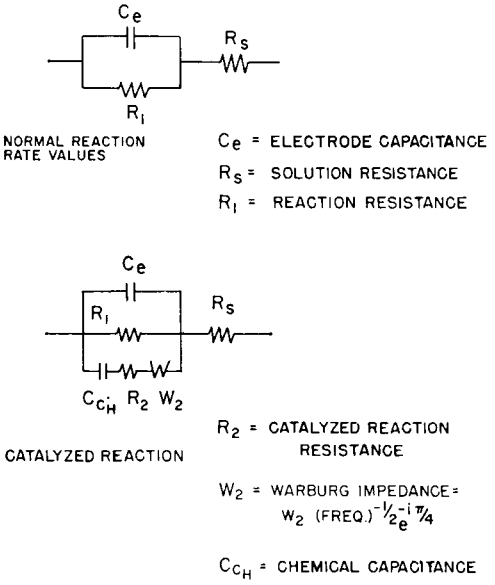

FIG. 15. Equivalent circuits for the impedance of polarized electrodes.

solutions obtained indicate that at audio and sub-audio frequencies the circuit of Figure 1 should well represent the electrode impedance. If a reaction occurring at the surface is well catalysed, a different behavior would be expected. There is little reaction resistance in such a case, but the depletion of the reacting species at the surface would require a diffusion of the ions to or away from the surface. This is responsible for an impedance which has the typical diffusion behavior and depends inversely on the square root of the frequency. It is called a Warburg impedance and is given the symbol W (Grahame 1952). The accumulation of the reaction product will in general tend to oppose any further reaction, and this causes an impedance just like that of a capacitance. We have given this capacitance the symbol C_{ch}. The equivalent circuits for an electrode impedance with normal reactions or with catalyzed reactions are shown in Figure 15.

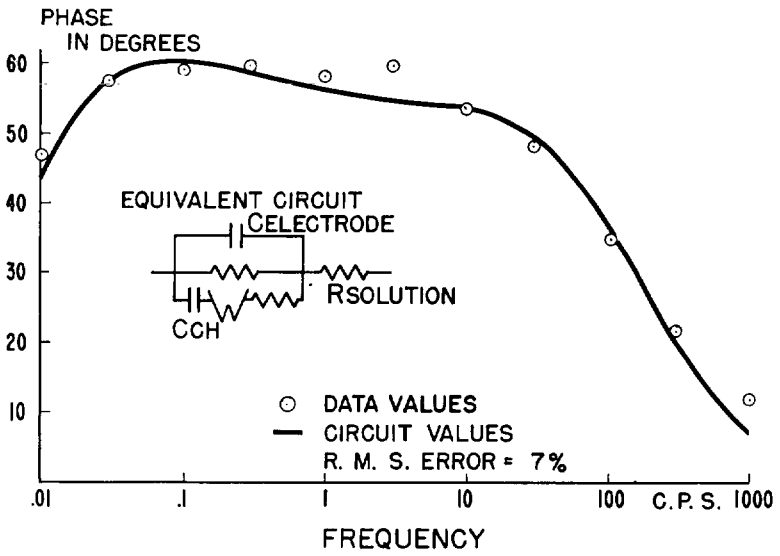

FIG. 16. Phase shift of the impedance of a magnetite electrode, and its comparison with the equivalent circuit.

Measurements were made on a wide variety of electrodes, and data were also obtained from the literature. Equivalent circuits such as those shown in Figure 15 were then adjusted to fit the data. In most cases the circuits could be made to fit the data within the experimental error. An example of such a fit is shown in Figure 16, where only the phase of the impedance is plotted. The magnitude of the impedance for this same electrode is shown in Figure 10, and on this logarithmic scale the errors of the equivalent circuit would not be discernible. The most striking result of these measurements was that in every case a well catalyzed reaction appeared to be taking place and contributed a large part of the current being passed. This means that the impedance was in a large part controlled by a diffusion phenomenon, just as in the membrane model. A summary of these electrode measurements is given in Table VI.

SUMMARY AND CONCLUSIONS

When using induced polarization measurements for the detection of metallic or semi-conducting minerals, one must be aware of other causes of the electrical polarization. An examination of the possible causes of these effects reduced the important factors to electromagnetic coupling effects and membrane polarization as well as the metallic mineral, i.e., electrode polarization that one is usually looking for. The electromagnetic effects can be avoided by using only information at very low frequencies. In typical mining exploration applications, one must work with frequencies of less than 10 cps.

TABLE VI

SUMMARY OF ELECTRODE IMPEDANCES

Values are given for 1 cm² of surface at room temp. Symbols are referred to Fig. 15.

Electrode	Reaction Resistance R_1	Electrode Capacitance C_e	Catalyzed Reaction Resistance R_2	Warburg Impedance W_2	Chemical Capacitance Cch
ST steel	160,000	3.2	11	3,960	247
Ni	8,500	112	3	670	830
Cu	3,080	3.8	19	1,270	55,000
Graphite	49,500	80	26	2,700	170
Pyrite	3,900	15.	60	800	150,000
Galena*	3,800	8.5	6	760	43,000
Magnetite*	222,000	4.8	101	5,870	106

* Area not known accurately.

Resistances given in ohms.
Capacities given in μf.
W_2 calculated at 1 cps.

The effects of membrane polarization are more difficult to separate out. The effects are more limited than the electrode polarization, but may still be significant. Detailed investigations of these two processes were made to look for fundamental differences in their electrical behavior. Unfortunately the investigations showed that the principal factor contributing to the electrode impedance is a diffusion phenomenon, and this is the same factor involved in membrane polarization. Both electrode and membrane impedances show a wide and gentle frequency variation making any discrimination on this basis very difficult. This result was borne out in the measurements on rock and clay samples. The phase shifts of the metal factor, which should represent approximately the phase shift of the blocked conduction paths, were computed from an analysis of transient measurements at one tenth, one and ten cps. for hundreds of samples. Although the results were often quite characteristic for a given rock or clay type, there seemed to be no clear separation between those samples with electrode polarization and those with membrane polarization. Some typical values are shown in Table VII.

This represents of course only a somewhat limited frequency range and a wider frequency analysis might prove to be more discriminating. It is difficult, however, to extend the measurements to higher frequencies in the field because of the electromagnetic coupling effects. The measurements at lower frequencies are in principle possible, but the natural earth currents make the noise problem an important practical factor.

The magnitude of the polarization effects still appears to be the best guide for the detection of electrode polarization in rocks. When the mineralized target is well below the surface, the observed effects are, of course, considerably reduced, and may be hardly different than a small background polarization. The authors are of the opinion that the greatest improvement in interpretation will come from

TABLE VII

METAL FACTOR PHASE IN DEGREES

Sample Type	Frequency cps.		
	10	1	0.1
Kaolinite	9	14	22
Mica	8	12	19
Ion exchange resins	13	29	51
Sediments from Colorado Plateau			
with sulphides	12	20	30
little or no sulphides	9	15	21
Sedimentary copper ore	12	18	19
Rhodesian copper ore	18	27	41
Field data, porphyry copper body		18	31
Lithic Tuff, little or no sulphides	12	22	34
Graphitic ss	13	16	22
Dirty sands from Dakota, ss sequence	11	17	30
Manganese ore	9	14	22
Highly magnetic altered, ultrabasic	42	41	47

an accurate handling of this geometric factor, rather than a subtle analysis of the frequency spectrum of the observed polarization.

ACKNOWLEDGMENTS

Much of this work was done under contract AT(05-1)-718 for the Raw Materials Division of the A.E.C., and we are very grateful for their support. We are also indebted to the M.I.T. Computation Center for the use of their I.B.M. 704 in carrying out the computations involved in the electrode equivalent circuit fitting, the membrane model impedance evaluation, and the Fourier analysis of the transient electrical data on rock samples.

All of our early work on induced polarization was done with fellow students, Phil Hallof, now at McPhar Geophysics, Keeva Vozoff, now at the University of Alberta, and Norman Ness, and their contributions are firmly entrenched throughout this paper. We also wish to acknowledge a fruitful interchange of ideas and information with Dr. A. A. Brant, whose group at Newmont Exploration Co., developed and carried out perhaps the first wide scale use of induced polarization, and Dr. Ralph Holmer and George Rogers of the Bear Creek Mining Co., whose group also has considerable field experience in these measurements. We are indebted to Hal Olsen and Professor Martin of the Civil Engineering Department for their help in carrying out and interpreting measurements on clay systems.

We also wish to acknowledge the cooperation of many groups and individuals who have sent us samples on request or have allowed us to make measurements on their properties. Among these are

A.E.C., Geophysics Research and Development Branch
Bear Creek Mining Co
Dome Exploration Ltd.

Calument and Hecla Mining Co.
National Lead Co.
Nucom Ltd.
Pan American Petroleum Corp.

REFERENCES

Bleil, D. F., 1953, Induced polarization, a method of geophysical prospecting: Geophysics, v. 18, p. 636–661.

Brant, A. A., personal communication.

Casagrande, L., 1952, Electro-osmotic stabilization of soils: Jour. Boston Soc. Divil Eng., v. 39, p. 51.

De Groot, S. R., 1951, Thermodynamics of irreversible processes: New York, Interscience Publishers.

Denbigh, K. G., 1951, The thermodynamics of the steady state: London, Methuen & Co., Ltd.

Eastman, 1928, Electromotive force of electrolyte thermocouples and thermocells and the entropy of transfer and absolute entropy of ions: J. Amer. Chem. Soc., v. 50, p. 292.

Eckart, 1940, Thermodynamics of irreversible processes: Phys. Rev., v. 58, p. 267.

Grahame, D. C., 1952, Mathematical theory of the faradaic admittance: Jour. of Electrochem. Soc., v. 99, p. 370.

Hallof, P., 1957, On the interpretation of resistivity and induced polarization results: Ph.D. thesis, M.I.T. Department of Geology and Geophysics.

Henkel, J. H., and Van Nostrand, R. G., 1957, Experiments in induced polarization: A.I.M.E. Trans., v. 9, p. 355–359.

Kermabon, A. J., 1956, A study of some electro-kinetic properties of rocks: M.S. thesis, M.I.T. Department of Geology and Geophysics.

MacDonald, J. R., 1953, Theory of A.C. space-charge polarization effects in photoconductors, semiconductors, and electrolytes: Phys. Rev., v. 92, p. 4.

Madden, Marshall, Fahlquist, and Neves, 1957, Background effects in the induced polarization method of geophysical exploration: A.E.C. report RME-3150.

Madden, T. R., and Marshall, D. J., 1958, A laboratory investigation of induced polarization: A.E.C. report RME-3156.

———, 1959, Electrode and membrane polarization A.E.C. report RME-3157

Olsen, H., 1958, Personal communication.

Schlumberger, C., 1920, Etude sur la prospection electrique du soussol: Paris, Gauthier-Villars, Chapt. VIII.

Sunde, E. D., 1949, Earth conduction effects in transmission systems: New York, D. Van Nostrand Co., Chapt. IV.

Uhri, D., 1958, Personal communication.

Vacquier, V., Holmes, C. R., Kintzinger, P. R., and Lavergne, M., 1957, Prospecting for ground water by induced electrical polarization: Geophysics, v. 22, p. 660–687.

Wirtz, V. K., 1948, Platzwechselprozesse in Flussigkeiten, *Zeit f. Naturforschung*, 3a, p. 672.

Wyllie, M. R. J., 1955, The role of clay in well-log interpretation: State of California, Division of Mines, Bulletin 169, p. 282.